



**HAL**  
open science

# The composite structure of mixed $\tau$ -(Ag, Cu) V<sub>2</sub>O<sub>5</sub> bronzes-Evidence for T dependant guest-species ordering and mobility

Wilfred Hermes, Mickaël Dollé, Patrick Rozier, Sven Lidin

► **To cite this version:**

Wilfred Hermes, Mickaël Dollé, Patrick Rozier, Sven Lidin. The composite structure of mixed  $\tau$ -(Ag, Cu) V<sub>2</sub>O<sub>5</sub> bronzes-Evidence for T dependant guest-species ordering and mobility. *Journal of Solid State Chemistry*, 2013, 199, pp.84 - 89. 10.1016/j.jssc.2012.11.029 . hal-04492713

**HAL Id: hal-04492713**

**<https://hal.science/hal-04492713v1>**

Submitted on 6 Mar 2024

**HAL** is a multi-disciplinary open access archive for the deposit and dissemination of scientific research documents, whether they are published or not. The documents may come from teaching and research institutions in France or abroad, or from public or private research centers.

L'archive ouverte pluridisciplinaire **HAL**, est destinée au dépôt et à la diffusion de documents scientifiques de niveau recherche, publiés ou non, émanant des établissements d'enseignement et de recherche français ou étrangers, des laboratoires publics ou privés.




## Open Archive Toulouse Archive Ouverte (OATAO)

OATAO is an open access repository that collects the work of Toulouse researchers and makes it freely available over the web where possible

This is a Publisher's version published in: <http://oatao.univ-toulouse.fr/25445>

**Official URL:** <https://doi.org/10.1016/j.jssc.2012.11.029>

**To cite this version:**

Hermes, Wilfred and Dollé, Mickaël and Rozier, Patrick  and Lidin, Sven  
*The composite structure of mixed  $\tau$ -(Ag, Cu) $_x$ V $_2$ O $_5$  bronzes—Evidence for  $T$  dependant guest-species ordering and mobility.* (2013) *Journal of Solid State Chemistry*, 199. 84-89. ISSN 0022-4596

Any correspondence concerning this service should be sent  
to the repository administrator: [tech-oatao@listes-diff.inp-toulouse.fr](mailto:tech-oatao@listes-diff.inp-toulouse.fr)

# The composite structure of mixed $\tau$ -(Ag, Cu)<sub>x</sub>V<sub>2</sub>O<sub>5</sub> bronzes Evidence for *T* dependant guest-species ordering and mobility

Wilfred Hermes<sup>a</sup>, Mickaël Dollé<sup>b</sup>, Patrick Rozier<sup>b</sup>, Sven Lidin<sup>a,\*</sup>

<sup>a</sup> Centre for Analysis and Synthesis (CAS), PO Box 124, Lund University, 221 00 Lund, Sweden

<sup>b</sup> Centre d'Elaboration de Matériaux et d'Etudes Structurales (CEMES-CNRS), UPR CNRS 8011, Université de Toulouse, 29, rue J. Marvig, BP 94347 31055, Toulouse Cedex, France

## ARTICLE INFO

**Keywords:**  
Cu,Ag bronze  
Modulated composite  
Ionic transport

## ABSTRACT

The complex structural behavior of  $\tau$  [AgCu]<sub>-0.92</sub>V<sub>4</sub>O<sub>10</sub> has been elucidated by single crystal X ray diffraction and thermal analysis. The  $\tau$  phase region is apparently composed of several distinct phases and this study identifies at least three:  $\tau_{1rt}$ ,  $\tau_{2rt}$  and  $\tau_{lt}$ .  $\tau_{1rt}$  and  $\tau_{2rt}$  have slightly different compositions and crystal habits. Both phases transform to  $\tau_{lt}$  at low temperature. The room temperature modification  $\tau_{1rt}$  crystallizes in an incommensurately modulated structure with monoclinic symmetry C2(0 $\beta$ 1/2) [equivalent to no 5.4, B2(01/2 $\gamma$ ) in the Intl. Tables for Crystallography, Volume C] and the cell parameters  $\mathbf{a}=11.757(4)$  Å,  $\mathbf{b}=3.6942(5)$  Å  $\mathbf{c}=9.463(2)$  Å  $\beta=114.62(2)^\circ$  and the  $\mathbf{q}$  vector (0 0.92 1/2), but it is more convenient to transform this to a setting with a non standard centering  $X=(1/2\ 1/2\ 0\ 0; 0\ 0\ 1/2\ 1/2; 1/2\ 1/2\ 1/2\ 1/2;)$  and an axial  $\mathbf{q}$  vector (0 0.92 0). The structure features a vanadate host lattice with Cu and Ag guests forming an incommensurate composite. The structural data indicates perfect Ag/Cu ordering. At low temperature this modification is replaced by a triclinic phase characterized by two independent  $q$  vectors. The  $\tau_{2rt}$  phase is similar to the low temperature modification  $\tau_{lt}$  but the satellite reflections are generally more diffuse.

## 1. Introduction

The versatility of vanadium in terms of accessible valence states (from +3 to +5), coordination number (4 to 6) and coordination polyhedral shapes (tetrahedron to octahedron with intermediate trigonal bipyramid) leads to the possibility to form a large variety of structure types in several chemical systems. These facts explain why vanadium oxide based compounds are widely studied as model compounds to define crystal chemistry parameters. In addition to structural versatility, vanadium presents attractive properties in different domains such as magnetism, catalysis and electrode materials for Li based batteries. More specifically, in addition to the conventional insertion process, (Ag,Cu) V O compounds present the displacement phenomenon which corresponds to the reduction of the Ag and Cu ions down to the metallic state associated with their extrusion out of the structure [1,2]. This specific behaviour has been observed in several groups of compounds such as (Ag,Cu) V O [3–7] (Ag,Cu)<sub>x</sub>-Mo<sub>6</sub>S<sub>8</sub> [8–10] AgCuO<sub>2</sub> delafossite [11,12] and is at the origin of the use of Ag<sub>2</sub>V<sub>4</sub>O<sub>11</sub> vanadate as active material in biomedical devices primary cells [13]. However, most of time, this phenomenon was reported as partial and irreversible. More recently, the

combination of insertion and displacement processes operating reversibly was shown for Cu<sub>7/3</sub>V<sub>4</sub>O<sub>11</sub> opening the way to a new class of active material known as Combined Displacement Insertion (CDI) electrodes [14]. Different studies allowed the definition of structural parameters responsible for the efficiency and reversibility of displacement phenomena [15,16]. The delocalization of the displaceable species over several crystallographic sites, none of them being either disallowed or ideally suitable, appears as one of the most important. One way to induce this delocalization is to mix, in a common host network, different displaceable species. For example,  $\delta$  Ag<sub>x</sub>V<sub>2</sub>O<sub>5</sub> and  $\epsilon$  Cu<sub>x</sub>V<sub>2</sub>O<sub>5</sub> are isostructural with the same [V<sub>4</sub>O<sub>10</sub>] double layer and with Ag<sup>+</sup> or Cu<sup>+</sup> ions localized in the interlayer space [17–21]. Volkov et al. [22] showed that mixed (Ag,Cu)V<sub>2</sub>O<sub>5</sub> compounds can be obtained and recently the average structure of the  $\tau$  (Ag<sub>0.45</sub>Cu<sub>0.45</sub>)V<sub>2</sub>O<sub>5</sub> compounds has been reported [23]. It presents the same [V<sub>4</sub>O<sub>10</sub>] double layer with Cu<sup>+</sup> ions fully delocalized along tunnels as shown using X ray diffraction. It was, however, obvious that the specific location of both silver and copper ions was subject to more complex structuring as also observed while studying the prototype Cu<sub>7/3</sub>V<sub>4</sub>O<sub>11</sub> structure [24,25]. The scope of the present paper is to describe more accurately the mixed  $\tau$ (Ag,Cu)<sub>x</sub>V<sub>2</sub>O<sub>5</sub> compounds to settle precise structural parameters allowing a full understanding of the relationship between the inserted species and their respective delocalization. We show that the system is in fact multi phasic, with structural transitions on cooling and we report

\* Corresponding author. Fax: +46 46 2228209.

E-mail address: Sven.Lidin@polymat.lth.se (S. Lidin).

on the full structure of the simplest of the phases present, the room temperature  $\tau_{1rt} [\text{AgCu}]_{\sim 0.92}\text{V}_4\text{O}_{10}$ .

## 2. Experimental

### 2.1. Synthesis

#### 2.1.1. Powdered samples

$\text{M}_x\text{V}_2\text{O}_5$  samples ( $\text{M}=\text{Ag}, \text{Cu}$  or a mixture of them) have been prepared following conventional solid state routes for mixed valence oxides. The reactants, Ag and Cu metal and  $\text{V}_2\text{O}_5$  were weighted in stoichiometric amounts to reach the desired composition. They were ground in an agate mortar and the mixture was placed in a quartz tube sealed under vacuum to avoid any risk of oxidation. To prevent any secondary reaction with quartz, a platinum foil isolated the mixture from the tube. The syntheses were performed at 620 °C for 12 h. The products were controlled by means of X ray diffraction before annealing under the same conditions to enhance both homogeneity and crystallinity of the samples.

#### 2.1.2. Single crystal growth

Powdered samples characterized as single phase materials were placed in a platinum crucible and heated, under vacuum, up to their melting point. The cooling rate was set to 1 °C/h until a temperature reaching 80% of the melting point. The sample was then cooled down to room temperature following the furnace inertia. In all cases, black, acicular single crystals were obtained. A part of the preparation was kept for further structural analysis while the rest of the sample was ground and analysed by XRD. This analysis confirms that the single crystals are representative of the powdered materials and indicate a congruent melting. The experimental pattern is also compared to the one calculated using results of the structure indicating that the selected single crystals are representative of the powdered samples.

## 3. Characterisation

### 3.1. Powder X ray diffraction

The samples obtained after each heat treatment were controlled by means of powder X ray diffraction using a Seifert 3000TT diffractometer with monochromatized Cu  $K_\alpha$  radiation ( $\lambda=1.5418 \text{ \AA}$ ). X ray patterns were measured in the  $5^\circ$ – $55^\circ$   $2\theta$  range in a step scan mode with a counting time of 4 s and an angular step width of  $0.02^\circ$   $2\theta$ .

### 3.2. Single crystal X ray diffraction

A single crystal was mounted on a thin glass fibre using epoxy resin and X ray diffraction data were collected at ambient conditions on an Oxford diffraction XCalibur III diffractometer using monochromatized MoKa radiation. All details pertinent to the data collection are given in the CIF file deposited as supporting information at the Bilbao crystallographic server, <http://www.cryst.ehu.es/>

### 3.3. Heat capacity measurement

The heat capacity measurement was carried out with a PPMS (Quantum design). Therefore the sample was fixed with Apiezon N grease and measured around the ordering temperature.

## 4. Results and discussion

### 4.1. Average structure

The average structure of  $\tau \text{Ag}_{0.5}\text{Cu}_{0.5}\text{V}_2\text{O}_5$  at room temperature [8] is described in the monoclinic system space group  $C2/m$  with cell parameters  $a=11.757(4) \text{ \AA}$ ,  $b=3.6942(5) \text{ \AA}$   $c=9.463(2) \text{ \AA}$   $\beta=114.62(2)^\circ$ . The structure is built up with  $\text{VO}_6$  octahedra sharing edges to form D4 type [26] double layers developed in the (0 0 1) plane (Fig. 1). The layers are stacked along the [0 0 1] direction in such a way that they define two kinds of tunnels. Each type of tunnel is filled with only one of the guest species leading to an ordered occupancy with alternatively copper or silver ions along the [1 0 0] direction. The copper ions are almost fully delocalised along their tunnel, but three main sites constitute the bulk of the electron density and correspond to alternatively octahedral and tetrahedral oxygen surroundings. The silver ions are slightly delocalised around their main site corresponding to a trigonal prismatic oxygen surrounding.

Since the experimental XRD powder pattern fits well with the calculated one, the studied sample appears to be single phase. The study of the thermal behaviour of the sample was investigated using DSC experiment. The evolution of the Cp versus  $T$  reported in Fig. 2 indicates a phase transition occurring at about 150 K. This transition spreads over an interval of several degrees which may indicate the existence of variable stoichiometry in the studied sample not distinguishable via powder XRD.

## 5. Preliminary studies

To go deeper in the understanding of the specific behavior of inserted species, X ray diffraction on single crystal is made. Despite no evidence on the basis of powder analysis, careful examination of the single crystals indicates the presence of two phases. The single crystals are all black and shiny but some present needle like and others platelet like shapes. It was not possible to obtain the product as single phase, and single crystals for the diffraction study were picked on the basis of color and habit. Preliminary single crystal diffraction experiments reveal subtle differences between the crystals with needle like habit and those that grow as platelets. For both compounds, X ray patterns (Fig. 3.) exhibit, in addition to main diffraction peaks, satellites indicative of modulation. In both cases, the main peaks are described with cell parameters about  $\mathbf{a} \approx 11.80 \text{ \AA}$ ,  $\mathbf{b} \approx 3.74 \text{ \AA}$ ,

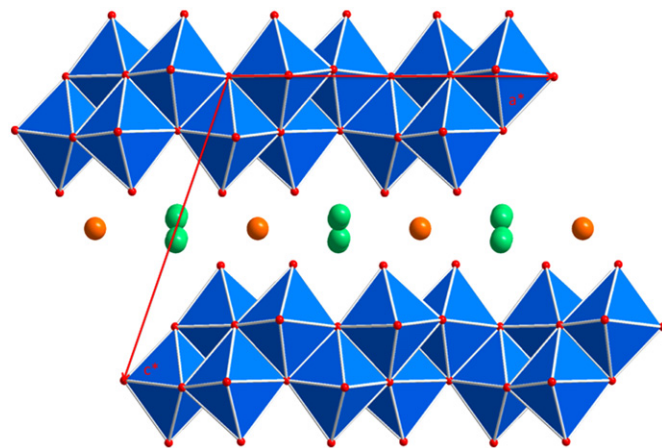


**Fig. 1.** Average structure of  $\tau\text{-(Cu,Ag)V}_2\text{O}_5$ : projection onto (0 1 0). Colour code: O red, Cu brown, Ag green, V in blue polyhedra. (For interpretation of the references to colour in this figure legend, the reader is referred to the web version of this article.)

$c \approx 18.92 \text{ \AA}$   $\beta \approx 114.6^\circ$  i.e., the basic unit cell typical for  $\tau$  VOB phases doubled along  $c$ . Despite such similarities, the modulation behavior is clearly different. The needles ( $\tau_{1rt}$ ) exhibit an arrangement of satellites typical for a composite structure, with a  $q$  vector of the form  $q_1 = (0.92 \ 0)$ , in a cell doubled along the  $c$  axis (Fig. 3 left). The platelets ( $\tau_{2rt}$ ) show a more complex pattern where the pairs of satellites  $(0.92 \ 0)$  and  $(0.08 \ 0)$  in the  $\tau_{1rt}$  phase are replaced by arcs of diffuse scattering (Fig. 3 center).

The thermal behavior of the sample, studied in the 135–293 K temperature range using Cp (Fig. 2), exhibits a transition occurring at about 150 K. The XRD data collected on each kind of single crystals below 150 K confirm the structural nature of the transition. At low temperatures both phases undergo a transition characterized by yet another, more complex, arrangement of satellite reflections (Fig. 3 right) that may be explained by two independent  $q$  vectors. For the  $\tau_{1rt}$  phase this entails that appearance of a new vector  $q_2$ , and a shift of the  $q_1$  vector of the RT phase to an off axis value, forcing triclinic symmetry. The circular diffuse scattering of the  $\tau_{2rt}$  phase breaks up into the same sets of satellites generated by two distinct  $q$  vectors. This confluence of the two RT phases into a single LT phase is probably due to the more restrictive structural constraints at low temperatures. What causes the differences between  $\tau_{1rt}$  and  $\tau_{2rt}$  is unclear, but it is most probably due to small differences in composition, since the

two crystal forms have identical thermal history. Further evidence is offered by the thermal behavior since a variable stoichiometry would explain the phase transition interval of several of degrees exhibited (Fig. 2).

The differences and similarities of the diffraction patterns are shown in Fig. 3.

Structural analysis of the  $\tau_{1rt}$  phase turned out to be relatively straight forward, while the  $\tau_{2rt}$  phase and the low temperature modification are more demanding. The satellites in the diffraction pattern of the  $\tau_{2rt}$  phase form an extended diffuse pattern and the low temperature modification exhibits very closely clustered spots that are difficult to resolve on an in house diffractometer.

In this paper, we will therefore concentrate on the structure of the  $\tau_{1rt}$  phase and only analyze the indexing problem of the low temperature phase, and hope to return to the enigma of the low temperature phase with the help of synchrotron diffraction experiment.

## 6. Structure of the $\tau_{1rt}$ phase

The diffraction pattern of the  $\tau_{1rt}$  phase is consistent with a monoclinic unit cell with the superspace group symmetry  $X2/m(0\beta 0)$ , the cell parameters  $a = 11.757(4) \text{ \AA}$ ,  $b = 3.6942(5) \text{ \AA}$ ,  $c = 18.926(4) \text{ \AA}$   $\beta = 114.62(2)^\circ$  and an axial  $q$  vector along  $b^*q = (0.92 \ 0)$ . An initial solution was produced using charge flipping in superspace [27,28], as implemented in the software system Superflip [29] and the model was refined using JANA2006 [30]. A model that accounts well for the weakly modulated vanadate part of the structure was easily produced (as reported earlier<sup>8</sup>), while the amplitudes of the modulations for the Ag and Cu positions are large. At this stage all atoms in the structure were treated using single harmonic displacive functions. In this model, Ag and Cu were not distinguishable from each other, but since both were clearly under occupied, occupational modulations on the Ag and Cu positions were introduced. This improved the fit between model and data, but the fit for the satellites still remained at unsatisfactory  $R$  values above 0.2. Inspection of the electron density maps of the coinage metal positions revealed a complex situation with a generally bad correspondence between the shape of the electron density and that of the modulation functions. This is typically a sign of a symmetry error and the two possible non centro symmetric monoclinic superspace subgroups  $X2(0\beta 0)$  and  $Xm(0\beta 0)$  were both tried. While refinement in the subgroup  $Xm(0\beta 0)$  yielded only a marginal improvement, refinement in  $X2(0\beta 0)$  dramatically improved the fit ( $R_{1satt} < 0.12$ ) between data and model. Electron density plots of the coinage

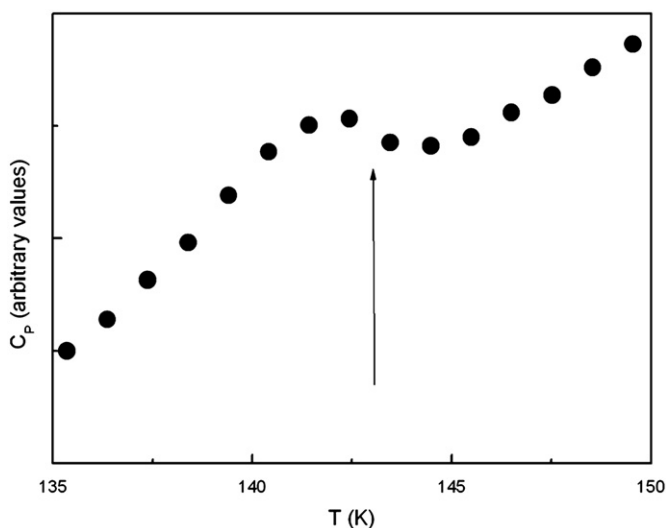


Fig. 2. Heat capacity measured as a function of temperature clearly shows the phase transition from  $\tau_{1rt}$  to  $\tau_{lt}$  that takes place between 140 and 145 K.

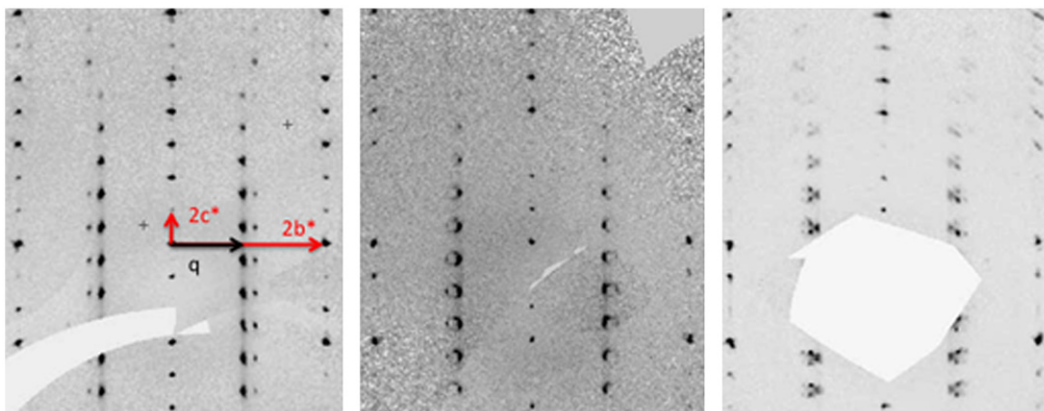


Fig. 3. Single crystal diffraction patterns of the 2 kl section of  $\tau_{1rt}$ -[AgCu]<sub>~0.92</sub>V<sub>4</sub>O<sub>10</sub> at room temperature (left),  $\tau_{2}$ -[Ag,Cu]<sub>x</sub>V<sub>4</sub>O<sub>10</sub> also at room temperature (centre) and  $\tau_{1lt}$ -[AgCu]<sub>~0.92</sub>V<sub>4</sub>O<sub>10</sub> at 100 K (right).



metal positions revealed saw tooth like behavior of both. This indicated that a composite model might be appropriate. The diffraction pattern in Fig. 3, left, corroborates this, in particular the marked difference in intensity between upstream and downstream satellites. A composite model was therefore introduced replacing  $b^*$  of the original reciprocal cell with  $q$  for the second composite part. The vanadate network was modeled, as previously, in the original cell, while the coinage metal positions were modeled in this second unit cell. The composite treatment is strictly formal and the scattering is produced by the two sub systems together, not as independent entities, but the composite description where a subset of the atomic positions are ascribed a separate unit cell is a compact and elegant way to model a positional and compositional modulation that would otherwise require many more parameters. When this was introduced, the refined occupancies of the mixed Ag/Cu positions converged to values indicating perfect ordering, and implementing this caused no detrimental effects to the fit.

The macroscopic sample is biphasic, and there are clearly at least two different ordering modes at room temperature,  $\tau_{1rt}$  and  $\tau_{2rt}$ . There is a risk that this is reflected also in the single crystal used for the measurement. It is a relatively common phenomenon for modulated phases that the ordering applies only to a partial volume of the crystal, and one ordering mode may continuously transform into another. In the final model a separate scale factor was introduced for the satellites to allow for part of the crystal to be disordered (or differently ordered) with respect to the intercalated coinage metals. This procedure produced an

improvement in the fit between model and data of 1.5% for  $R_{1main}$  and 3% for  $R_{1satt}$ . This final model shows an excellent agreement between data and model ( $R_{1main}=0.036$ ,  $R_{w(F2)main}=0.098$ ,  $R_{1sat}=0.074$ ,  $R_{w(F2)sat}=0.14$ ) using 110 parameters refined against 3246 unique (2264 observed) reflections. All details of the refinement may be found in the CIF of the supporting information.

The modulations of the vanadate part are small and sinusoidal, while the coinage metals behave in a more intricate way. The Cu atom position is restricted by symmetry to be subject to a displacive modulation along the unique axis only, and this displacement is small (confer Fig. 4, left), while the displacive modulation of Ag is more complicated. Fig. 4, right shows a bounded sum (2 Å thickness) perpendicular to the  $ab$  plane. The electron density of the Ag atom clearly exhibits a discontinuous behavior with two identical sets of maxima with a relative displacement of  $1/2$  along  $b$ . Those are also strongly displaced in the projection direction across the two fold axis of rotation and the two maxima are, in fact, symmetry equivalent with respect to the two fold axis and a  $1/2$  translation along internal space. The specific atomic surface of the model (red) therefore only covers half of the maxima indicated in the image. The displacive modulation function of Ag is modeled using a saw tooth function and a single harmonic on top of that. Note that the principal axis of the electron density ellipsoids of the Ag position is inclined to the internal space direction at an angle equal to that of external space. This indicates that the Ag position may equally well be modeled as located in composite part 1. This is indeed possible, but leads to a partial occupancy of this position. The model

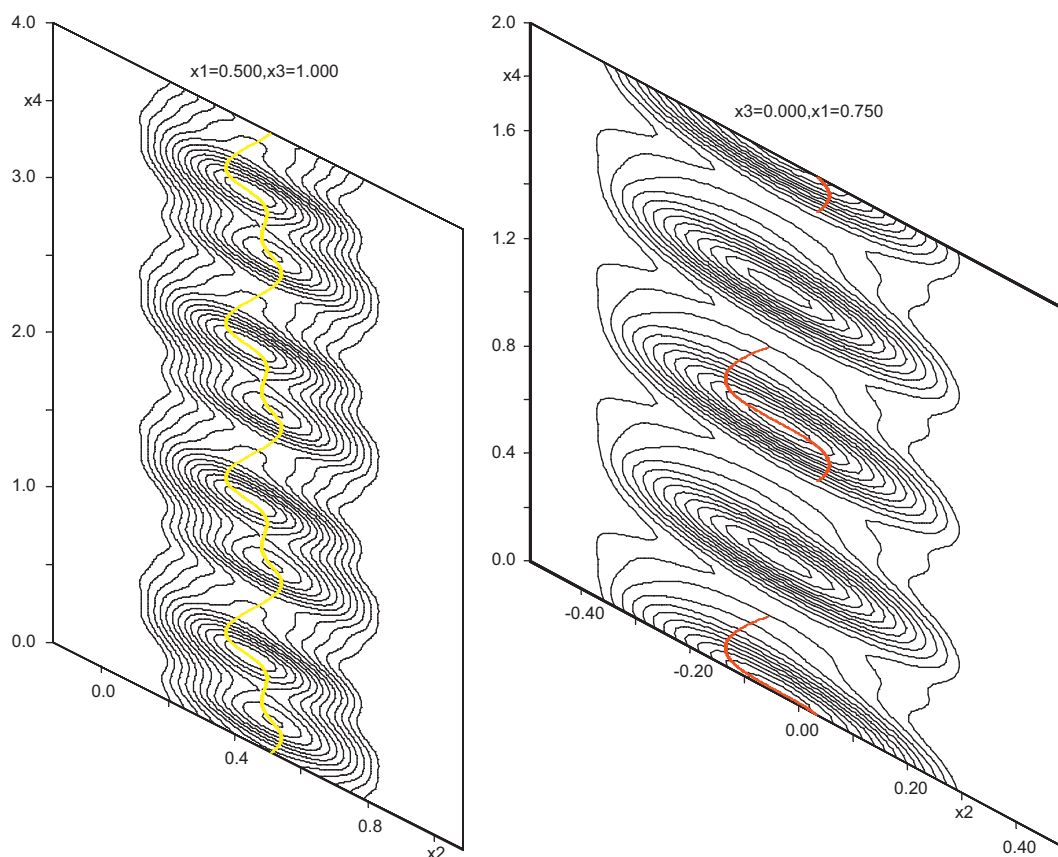


**Fig. 4.** Electron density plots showing the modulation functions of Cu (left) and Ag (right). The map on the left is a section. Since the Cu position is constrained by symmetry and no modulation is allowed along the perpendicular directions, this section contains all pertinent information. The Ag position is subject to a substantial modulation along  $c$ , and here the map is a bounded projection along  $c$  to capture the behavior of the silver atom over the range of  $c$ . The red trace shows the model of the Ag position. The part of the electron density that appears to be un-modelled is the symmetry equivalent electron density on the far side of the 2-fold axis. This behavior is also clear from the real space structure in Fig. 5. The corresponding residual electron density maps are essentially featureless with maxima and minima around  $1 \text{ e}/\text{\AA}^3$ . (For interpretation of the references to colour in this figure legend, the reader is referred to the web version of this article.)



structures can be accurately studied as the second one shows diffuse satellites tricky to index. Both compounds confluence at low temperature to the same structure however impossible to fully characterize using in house diffractometer. Nevertheless, the refinement of the  $\tau_1$  structure clearly evidence the composite character of the structure and underline the large and almost continuous shift of both Cu and Ag ions along tunnels in between  $V_2O_5$  layers. While copper move along a straight line through edge sharing octahedra and tetrahedra, silver diffusion pathway occurs in a zig zag way between trigonal prism. This precise analysis allows then to indicate that despite exhibiting identical average structure the modification of the composition about the nominal 1/2 1/2 leads to subtle structural changes and that, instead of what determined using average structure, both ions appears mobiles. These findings allow explaining that both cations are subjected to displacement phenomena when reacted with lithium and by the way confirm the direct relationship between cation site stability and their mobility and reactivity.

### Acknowledgment

This research was sponsored by the VR. W. H. is grateful to the DAAD for a Post Doc fellowship.

### Appendix A. Supporting information

Supplementary data associated with this article can be found in the online version at <http://dx.doi.org/10.1016/j.jssc.2012.11.029>.

### References

- [1] K.D. Kepler, J.T. Vaughey, M.M. Thackeray, *Electrochem. Solid-State Lett.* 2 (1999) 307.
- [2] R. Brec, E. Prouzet, G. Ouvrard, J. Power Sources 43–44 (1993) 277–288.
- [3] F. Garcia-Alvarado, J.M. Tarascon, *Solid State Ionics* 73 (1994) 247.
- [4] M. Eguchi, T. Iwamoto, T. Miura, T. Kishi, *Solid State Ionics* 89 (1996) 109–116.
- [5] Y. Sakurai, J.-I. Yamaki, *Electrochim. Acta* 34 (1989) 355–361.
- [6] D. Ilic, D. Neumann, J. Power Sources 43–44 (1993) 589–593.
- [7] M. Giorgetti, S. Mukerjee, S. Passerini, J. McBreen, W.H. Smyrl, J. *Electrochem. Soc.* 148 (2001) A768–A774.
- [8] Y. Takeda, R. Kanno, M. Noda, O. Yamamoto, *Mater. Res. Bull.* 20 (1985) 71–77.
- [9] W.R. McKinnon, J.R. Dahn, *Solid State Commun.* 52 (1984) 245–248.
- [10] J.-M. Tarascon, T.P. Orlando, M.J. Neal, J. *Electrochem. Soc.* 135 (1988) 804–809.
- [11] C.D. May, J.T. Vaughey, *Electrochem. Commun.* 6 (2004) 1075–1079.
- [12] F. Sauvage, D. Munoz-Rojas, K.R. Poeppelmeier, N. Casan-Pastor, J. *Solid State Chem.* 182 (2009) 374–380.
- [13] R.A. Leising, E.S. Takeuchi, *Chem. Mater.* 6 (1994) 489.
- [14] M. Morcrette, P. Rozier, L. Dupont, E. Mugnier, L. Sannier, J. Galy, J.-M. Tarascon, *Nat. Mater.* 2 (2003) 755–761.
- [15] P. Poizot, F. Chevallier, L. Laffont, M. Morcrette, P. Rozier, J.M. Tarascon, *Electrochem. Solid-State Lett.* 8 (4) (2005) A184–A187.
- [16] P. Rozier, M. Morcrette, O. Szajwaj, V. Bodenez, M. Dolle, C. Surcin, L. Dupont, J.M. Tarascon, *Isr. J. Chem.* 48 (3–4) (2008) 235–249.
- [17] S. Andersson, *Acta Chem. Scand.* 19 (1965) 1265–1369.
- [18] S. Andersson, *Acta Chem. Scand.* 19 (1965) 1371–1375.
- [19] J. Galy, D. Lavaud, A. Casalot, P. Hagenmuller, J. *Solid State Chem.* 2 (1970) 531–543.
- [20] A. Casalot, A. Deschanvres, P. Hagenmuller, B. Raveau, *Bull. Soc. Chim. Fr.* 6 (1965) 1730–1731.
- [21] A. Casalot, M. Pouchard, *Bull. Soc. Chim. Fr* 10 (1967) 3817–3820.
- [22] V.L. Volkov, B.G. Golovkin, *Russ. J. Inorg. Chem.* 33 (1988) 1043–1044.
- [23] P. Rozier, M. Dollé, J. Galy, J. *Solid State Chem.* 182 (2009) 1481–1491.
- [24] R. Withers, P. Rozier, *Z. Kristallogr.* 215 (2000) 688–692.
- [25] P. Rozier, S. S. Lidin, J. *Solid State Chem.* 172 (2003) 319–326.
- [26] J. Galy, J. *Solid State Chem.* 100 (1992) 209–245.
- [27] G. Oszlanyi, A. Suto, *Acta Crystallogr. A* 60 (2004) 134–141.
- [28] G. Oszlanyi, A. Suto, *Acta Crystallogr. A* 61 (2005) 147–152.
- [29] L. Palatinus, G. Chapuis, J. *Appl. Crystallogr.* 40 (2007) 786–790.
- [30] Petricek, V., Dusek, M. and Palatinus L., Institute of Physics, Academy of Sciences of the Czech republic of Science, 2006.